İSTANBUL UNIVERSITY CERRAHPAŞA

ORIGINAL ARTICLE
Electrica 2023; 23(1): 48-60

Modelling, Validation, and Simulation of Solar Photovoltaic Modules

Alhassan Ali Teyabeen[1], Ali Elseddig Jwaid[2]

[1]Libyan Center for Solar Energy Research and Studies, Tripoli, Libya
[2]Faculty of Computing, Engineering and Media, De Montfort University, UK

Cite this article as: A. Ali Teyabeen and A. Elseddig Jwaid, "Modelling, validation, and simulation of solar photovoltaic modules," *Electrica*, 23(1), 48-60, 2023.

ABSTRACT

Modelling of solar photovoltaic (PV) systems which convert the sunlight into electricity require taking weather data as input variables, such as solar radiation and temperature, the output of the system can be considered as electrical power. The change in the input of the solar PV system will cause a change in the output of the system. In this paper, modelling of solar PV modules based on double-diode model equivalent circuit was achieved using MATLAB script by estimating parameters of the non-linear *I-V* curve using Newton-Raphson method by adjusting the non-linear *I-V* curve at three points: maximum power, open circuit voltage, and short circuit current. The established non-linear model allows predicting the behaviour of solar PV modules under different physical and environmental factors. The established model was validated by comparing its predicted performance with measured data of KYOCERA KC125GT solar PV module recorded at the field. The accuracy of the model performance was evaluated using statistical error tests such as root mean square error, RMSE, and correlation coefficient, R^2. The results showed that there is a good agreement between measured and predicted data. The performance of the predicted model used for simulation of the effect of variation of environmental factors such as solar radiation and temperature, and physical parameters such as series and parallel resistances. The simulation results show that the increase in solar radiation will result in an increase in harvested power, and the increase in temperature will result in a decrease in harvested power.

Index Terms—Solar photovoltaic energy, PV parameters extraction, double-diode model, modelling and simulation, performance evaluation, outdoor experiment

I. INTRODUCTION

Solar PHOTOVOLTAIC (PV) systems generate electricity by converting sunlight into electricity. The basic component of a PV system is the solar PV cell; it requires semiconductor processing techniques in order to be manufactured at low cost and high efficiency. The grouped cells form a module (panel). The module contains many cells connected in series to get large output voltage, whereas a large output current at terminals of the module can be achieved by connecting the cells in parallel, or by increasing the cells surface area. A PV array is a set of modules connected together in series and parallel to achieve the desired voltage and current to form a large PV system. The solar photovoltaic module produces DC electricity, it may uses to feed small loads like DC motors or lighting. More sophisticated applications requiring AC electricity, the DC/AC inverters are implemented in solar PV systems. The output of a PV system is influenced by environmental factors, and even the physical nature of the cell, but it mainly depends on environmental factors, especially solar radiation and temperature. The irradiation primarily affects the amount of current produced, and temperature controls the voltage produced. All of these factors need to be taken into consideration to know the behaviour of *I-V* curve and then accurately predict the PV energy production. The current-voltage relationship of a solar PV module is described by a mathematical model that is both implicit and nonlinear.

Several studies have investigated modelling and simulation of the effects of environmental and physical factors on the performance of PV devices using MATLAB. Salmi et al. [1] proposed a model based on single-diode using MATLAB/Simulink to study the behaviour of PV cell under different physical and environmental factors. The study also validated the MATLAB/Simulink model by comparing it with experimental results got from the solar panel. Kumar et al. [2] tested the behaviour of the single diode model created using MATLAB/Simulink on the performance of PV cell by comparing the characteristics of *I-V* curve obtained using the developed model with experimental values, they also studied the effect of environmental and physical factors on the performance of PV cell. Álvarez et al. [3] Modeled the behaviour of solar PV module/cell using single-diode/2-resistance equivalent circuit. Lambert W-function was used to extract the

Corresponding author:
Alhassan Ali Teyabeen

E-mail:
alhassan.teyabeen@gmail.com

Received: December 6, 2021

Revised: February 20, 2022

Accepted: April 15, 2022

Publication Date: July 27, 2022

DOI: 10.5152/electrica.2022.21164

parameters of solar PV devices. The results showed that there is high accuracy for the presented methodology in estimating the solar PV parameters. The studies in the literature used an equivalent electrical circuit to describe the PV device based on single diode [4–7] and double diode [8, 9]. To solve the non-linear I-V equation, different methods were proposed in the literature. Some of the studies presented the Gaussian Iteration method [10, 11]. Lambert W-function was also presented to solve *I-V* equation [3, 12–17]. While other studies used the Newton-Rapson method [6, 9, 18, 19].

Nomenclature		N_s	Number of cells connected in series
FF	Fill factor	N_p	Number of cells connected in parallel
G	Irradiance (W/m^2)	P_{max}	Maximum power (W)
I	PV output current (A)	*q*	Electron charge (C)
I_0	Reverse saturation current (A)	R_s	Series resistance (Ω)
I_{ph}	Photogenerated current (A)	R_{sh}	Shunt resistance (Ω)
I_{sc}	Short circuit current (A)	STC	Standard test condition
I_{mp}	Current at MPP (A)	*T*	Temperature (Kelvin)
k	Boltzmann constant (J/k)	T_{amb}	Ambient temperature (°C)
K_I	Temperature coefficient of I_{sc} (A/K)	*V*	PV output voltage (V)
K_V	Temperature coefficient of V_{oc} (V/K)	V_{mp}	Voltage at MPP (V)
MPP	Maximum power point	V_{oc}	Open circuit voltage (V)
n	Ideality diode factor	V_T	Thermal voltage (V)
NOCT	Nominal operating cell temperature	η_{max}	Maximum efficiency

Although several studies were reported on the description of solar photovoltaic devices performance[1, 2, 20–23], there were limitations that the second diode element is not included in the mathematical model. The single diode model does not represent a type of recombination that occurred in the PN junction which can be represented by the second diode [24]. This type of recombination has an effect on the voltage at the terminals of practical solar PV devices. It found that the double-diode model exhibits better accuracy than the single-diode model [25].

Some of the studies in the literature extracted the non-linear parameters of the solar cell [26]. But due to the non-linear relationship between the characteristics of solar PV cell and solar PV module composed of a number of *N* of cells, it can't multiply the values of extracted cell parameters by *N* to get module parameters, because there is a connection resistance between the connected cells, moreover, there is a slight difference between the solar PV cells during fabrication. So there is a need to extract the parameters of the solar PV module.

The purpose of this paper is to estimate the parameters of nonlinear *I-V* curve of the photovoltaic panel based on double-diode equivalent circuit, and also to introduce the behaviour of solar photovoltaic panels under different physical factors and various weather conditions by applying a mathematical model developed using double-diode equivalent circuit. Also to reach to the equations which explain the effect of the mentioned factors on the solar photovoltaic panel performance without intention of a detailed analysis of the semiconductor physics. The MATLAB script file program is used for simulation, which uses Newton-Raphson's method to solve current-voltage relationship numerically.

This paper is organized as follow. Section 2 presents the mathematical model of a solar PV cell, module, and array based on both one-diode and two-diode diode. Section 3 presents the components of *I-V* curve. Section 4 describes mathematically the effects of weather factors such as irradiation and temperature as well as the physical factors of solar cell on the performance of solar PV module. Section 5 introduces a numerical technique to estimate the parameters of solar PV module. Section 6 offers statistical error tests used to evaluate the performance of the model. Section 7 illustrates the simulation results of the effects on the PV module.

II. MODELLING OF PV DEVICES

Several mathematical models to describe photovoltaic devices from simple to more complex models are existed. In this paper, three models are presented.

A. Ideal Solar PV Cell

An ideal solar cell consists of one diode connected in parallel with photo-generated current (photo current, I_{ph}) as shown in Fig. 1. The current-voltage (*I-V*) relationship of the ideal photovoltaic cell can be mathematically described, given as [18, 27, 28]:

$$I = I_{ph,cell} - I_{0,cell}\left(e^{\frac{V}{nV_T}} - 1\right) \quad (1)$$

where $I_{ph,cell}$ (in Amperes) is the photogenerated current of the solar cell, it is directly proportional to the solar radiation, I_D is the diode current (in Amperes), $I_{0,cell}$ is the diode reverse saturation current, *e* is the exponential function, *n* is the diode ideality factor (ideal value is 1), *V* is terminal voltage (in volts), and V_T (in volts) is the thermal voltage of the cell, it's given by [18]:

$$V_T = \frac{kT}{q} \quad (2)$$

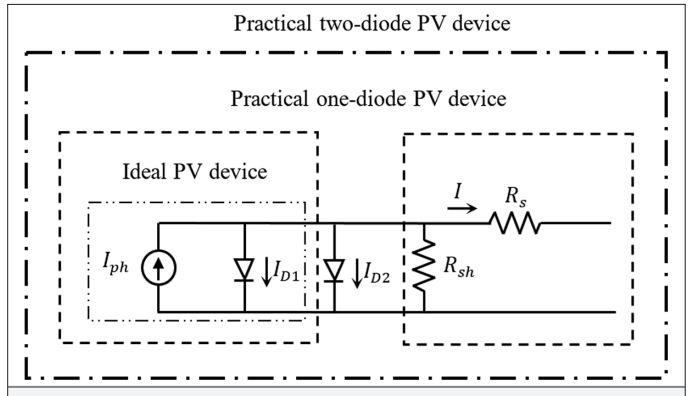

Fig. 1. Equivalent circuit of a practical PV device.

where T is the temperature(in Kelvin) of the p–n junction, k is the Boltzmann constant (1.38064×10^{-23} J/K), and q is the electron charge (in coulomb) equals 1.6021×10^{-19} C [18].

B. Single-Diode Mathematical Model

The equation of a solar PV cell presented in (1) doesn't represent the current-voltage (*I-V*) characteristics of a practical solar PV device which requires including additional parameters to the basic equation. The equivalent circuit of one diode mathematical model for solar PV devices is shown in Fig. 1 with ignoring the second diode, its mathematical equation can be represented by (3). The circuit consists of a series resistance R_s and a shunt resistance R_{sh} in parallel with a diode. The series resistance is the losses of series resistive, which are presented in the practical solar cell, and the reason of existence (representation) of shunt resistance is the reverse saturation current at the p-n junction, it depends on the method of fabrication of the solar PV cell. Generally, the value of series resistance is very low, and the value of shunt resistance is high [18]. The output current shown in Fig. 1 is given by [12, 18, 29–34]:

$$I = I_{ph} - I_0\left(e^{\frac{V+R_sI}{nV_T}} - 1\right) - \frac{V+R_sI}{R_{sh}} \tag{3}$$

C. Double-Diode Mathematical Model

The equivalent (electrical) circuit of double-diode mathematical model for solar PV devices is illustrated in Fig. 1, [9, 19, 35–37] its mathematical equation can be represented by (4). This model describes the effect of carriers recombination (which is presented by the second diode), it is also more accurate than one diode model, thus it adds further complexity [25, 35]:

The mathematical equation that describes the current-voltage (*I-V*) relationship which is got from the double diode equivalent circuit is given by [9, 19, 35]

$$I = I_{ph} - I_{01}\left(e^{\frac{V+R_sI}{n_1V_T}} - 1\right) - I_{02}\left(e^{\frac{V+R_sI}{n_2V_T}} - 1\right) - \frac{V+R_sI}{R_{sh}} \tag{4}$$

where I_{ph} (in Amperes) is the photogenerated current, I_{01} and I_{02} are the saturation currents of diode D_1 and D_2, respectively. n_1 and n_2 are the ideality factor of diode D_1 and D_2, respectively. There is a so-called "short circuit current", it's the maximum available current at the practical solar PV device terminals, at short circuit condition which means zero output voltage ($I = I_{sc}$, $V = 0$), also by ignoring second and third terms in the right-hand side of (4) for their very small values, yield [18, 34]

$$I_{sc} = I_{ph}\frac{R_{sh}}{R_s + R_{sh}} \tag{5}$$

The series resistance value is very low and the value of shunt resistance is high in practical solar cells, so the assumption of $I_{sc} \approx I_{ph}$ can be used in the modelling of solar PV devices [18, 38]. The reverse saturation current I_0 is affected by temperature variation as follow: [9, 18, 19]

$$I_{01} = \frac{I_{sc,STC} + K_I\Delta T}{\exp\left[\left(V_{oc,STC} + K_V\Delta T\right)/\left(n_1V_T\right)\right] - 1} \tag{6}$$

$$I_{02} = \frac{I_{sc,STC} + K_I\Delta T}{\exp\left[\left(V_{oc,STC} + K_V\Delta T\right)/\left(n_2V_T\right)\right] - 1} \tag{7}$$

where $I_{sc,STC}$ (in amperes), and $V_{oc,STC}$ (in volts) represent the short circuit current and open circuit voltage at standard test condition (STC), respectively. At STC an irradiance is 1000 W/m^2 with an AM 1.5 spectrum at 25°C [18]. AM stands for air mass, it defines the light spectrum (spectral distribution of the solar reference irradiance). K_I, K_V, are the temperature coefficients of short circuit current and open circuit voltage respectively. ΔT is the difference (Kelvin) between the actual cell temperature (in Kelvin) and the temperature at STC (in Kelvin), ($\Delta T = T - T_{STC}$). In fact I_{01}, and I_{02} are not function of irradiance because $I_{sc,STC}$ shown in (6) and (7) describes the short circuit current at STC, thus I_{01}, and I_{02} are independent of irradiance.

If the panel (module) is composed of a number of N_s cells connected in series and number of N_P cells connected in parallel, then $V_T = N_s \times kT/q$ is the equivalent thermal voltage of the panel (module), $N_s \times R_s$ is the module equivalent series resistance, and $N_s \times R_{sh}$ is the equivalent shunt resistance [18, 31]. Also, the photo and saturation currents expressed as $I_{sc} = N_p \times I_{sc,cell}$, $I_0 = N_P \times I_{0,cell}$ respectively. So, for a PV module composed of N_s cells connected in series and N_p cells connected in parallel, the current-voltage relationship (4) can be rewritten as:

$$I = I_{sc} - I_{01}\left(e^{\frac{V+R_sI}{n_1V_T}} - 1\right) - I_{02}\left(e^{\frac{V+R_sI}{n_2V_T}} - 1\right) - \frac{V+R_sI}{R_{sh}} \tag{8}$$

where I_{sc} (in Amperes) is the module short circuit current, it usually given in datasheet, R_s (in Ω) is the module series resistance, and R_{sh} (in Ω) is the module shunt resistance. The model given in (8) can be used not only for a PV module, but also for a PV array including several PV modules, or even a single cell ($N_s = 1$, $N_p = 1$). Henceforward the term "module" will be used to indicate to the PV device since the datasheet gives information about module composed of many cells connected in series and parallel.

In fact, cells are covered with anti-reflective coating, when they are mounted into modules, then they will have a temperature different to (higher than) ambient temperature. The nominal operating cell temperature (NOCT) is the temperature of the cells mounted in the module which will reach when the cells operated at irradiance 800 W/m^2, temperature of ambient of 20°C, AM 1.5, and a wind speed of 1 m/s. The cell temperature T_{cell} (in °C) can be estimated as [39, 40]:

$$T_{cell} = T_{amb} + \left(\text{NOCT} - 20\right) \times \frac{G}{800} \tag{9}$$

where T_{amb} is the ambient temperature (in °C), NOCT usually informed in the datasheet, and G is the irradiation (in W/m^2). It can be clearly seen from (9) that, at fixed ambient temperature the increase in irradiation will result in an increase of the cell temperature.

The *I-V* curve illustrated in Fig. 2 originated by using equation (8) using steps illustrated in the flowchart in Fig. 3. As can be seen in Fig. 2, three remarkable points are highlighted: short circuit current point (0, I_{sc}), open circuit voltage point (V_{oc},0), and maximum power point (V_{mp},I_{mp}). The *I–V* characteristics of the solar PV module

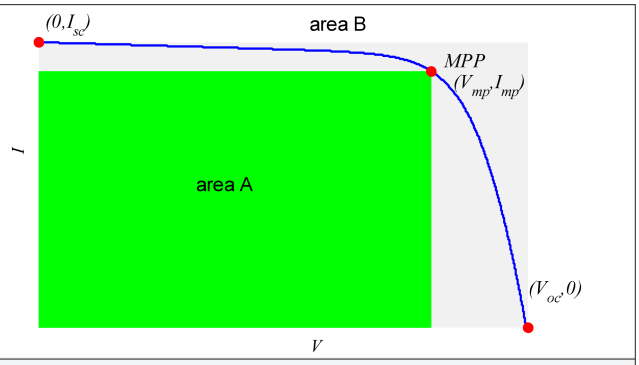

Fig. 2. curve of I–V characteristic of a practical PV device, where three remarkable points: short circuit point (0, I_{sc}), open circuit point (V_{oc}, 0), and MPP (V_{mp}, I_{mp}).

are influenced by the internal characteristics of the device (R_s, R_{sh}, I_{01}, I_{02}, n_1, n_2) and the external factors, such as irradiance *G*, and temperature *T*. The incident light directly affects the current generated by the device, and the temperature affects the terminal voltage of the device. The simulation in this paper to get the curves of *I-V* and *P-V* characteristics will be achieved by using double diode model (8).

Instead of the *I–V* curve equation, manufacturers of the solar PV devices support some of the experimental data about thermal and electrical characteristics of the modules, which is known datasheet. Datasheet of the module contains its specification, and it provides information about its performance according to STC. The specification of the KYOCERA KC125GT polycrystalline solar PV panel (module) is illustrated in Table I. Some of the experimental data provided in the datasheet are components of *I-V* curve. the following section presents the components of *I-V* curve.

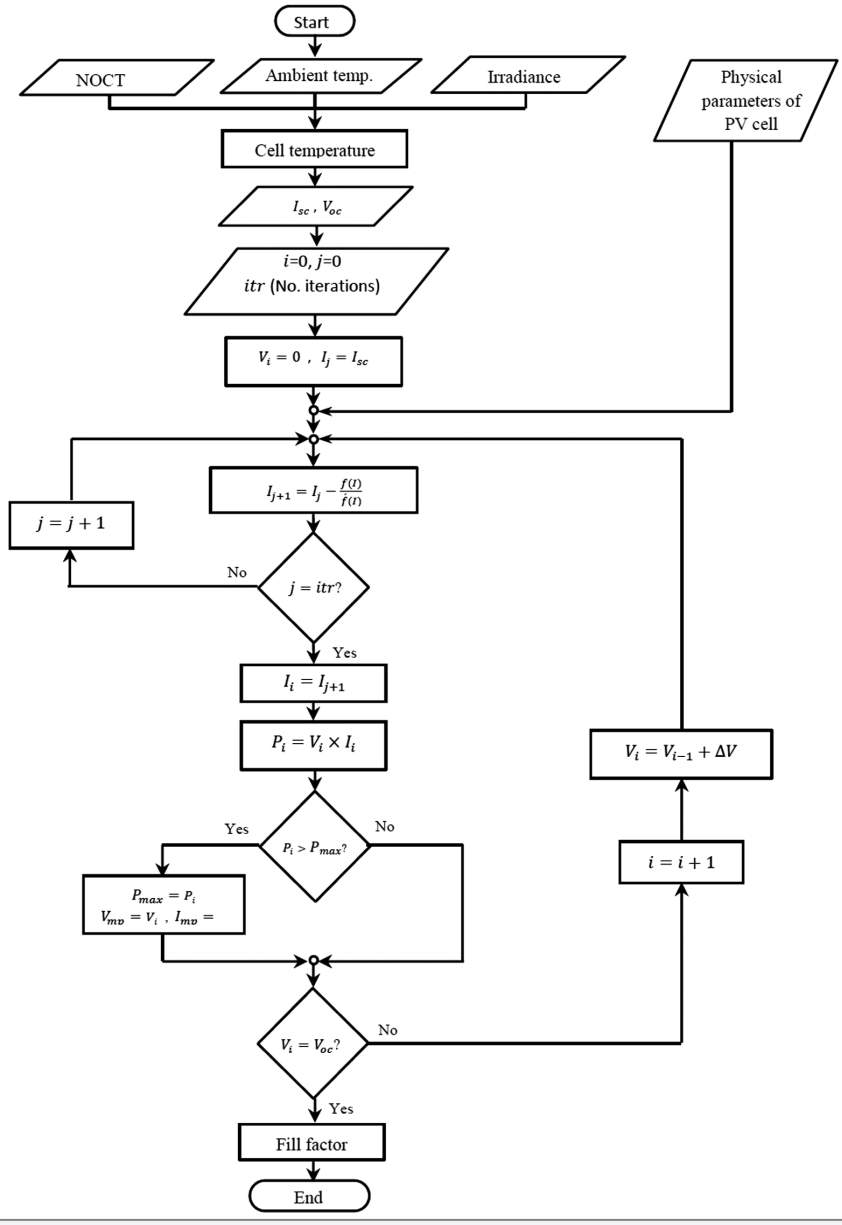

Fig. 3. Flowchart for determining the electrical characteristics of a solar PV module.

TABLE I. SPECIFICATIONS OF KYOCERA KC125GT POLYCRYSTALLINE SOLAR PV MODULE

Electrical characteristics	
Maximum power (P_{max})	125 Wp
Open circuit voltage (V_{oc})	21.7 V
Optimum operating voltage (V_{mp})	17.4 V
Short circuit current (I_{sc})	8.0 A
Optimum operating current (I_{mp})	7.2 A
Module efficiency (η_{max})	16.40 %
Thermal characteristics	
Temperature coefficient of I_{sc} (K_I)	0.00318 %/°C
Temperature coefficient of V_{oc} (K_V)	-0.0821 %/°C
Component materials	
Cells per module	36
Cell type	polycrystalline

III. COMPONENTS OF *I-V* CURVE

The components of *I-V* curve which are clearly seen in Fig. 2 and informed in the datasheet are the following:

A. Short Circuit Current

The first important element in the characteristics of solar PV devices is the short circuit current I_{sc}, which is represented in *I-V* curve by a point called short circuit point, this point is originated when the non-linear *I-V* curve crosses the current axis (y-axis). The value of current at this point is called the short circuit current. It is informed in the datasheet at STC.

Moreover, datasheets usually inform the short circuit current at other cases such as 800 W/m^2, NOCT, AM 1.5, this value is lower than the $I_{sc,STC}$ because the short circuit current of the solar PV module is influenced (linearly depends) by the solar radiation. The temperature affects the short circuit current according to the following equation [9, 18, 19, 21]:

$$I_{sc} = \left(I_{sc,STC} + K_I \Delta T\right)\frac{G}{G_{STC}} \tag{10}$$

where G and G_{STC} are the actual irradiance on the surface of module and the irradiance at standard test condition, respectively, (both in Watts per square meters). K_I is informed in datasheet.

B. Open Circuit Voltage

The second important element in the characteristics of solar PV devices is the open circuit voltage V_{oc}, which is represented in the *I-V* curve by a point called open circuit point, this point is originated when the non-linear *I-V* curve crosses the voltage axis (y-axis). The voltage value at this point is called the open circuit voltage, it is informed in the datasheet at STC, it's known as the nominal open circuit voltage, it is the maximum value available at terminals of a practical module at STC. Also, datasheets usually inform the open circuit voltage at the case of 800 W/m^2, NOCT, AM 1.5. However, the datasheet may inform *I-V* characteristics at other conditions. Applying the condition of open circuit point,(V_{oc},0), to the *I-V* expression (8) and ignoring both third and fourth terms on the right-hand side for simplicity, yield [27, 41]:

$$V_{oc} = V_T In\left(1 + \frac{I_{sc}}{I_0}\right) \tag{11}$$

It can be clearly seen from (11) that the relation between the ratio of I_{sc}/I_0 and open circuit voltage is logarithmic relation, and it is noted that the short circuit current scales linearly with irradiance as clarified in (10), thus at constant temperature the V_{oc} scales logarithmically with irradiance. So it can be noted that the increase in irradiance caused a logarithmic increase (little change) in the open circuit voltage. Therefore, it can be perceivable that the solar irradiance affects the short circuit current much larger than the open circuit voltage.

On the other side, under constant irradiance the increasing temperature (the influence of $V_T = kT/q$ can be ignored because the value of k is very small) caused increasing saturation current I_0, which in turn caused decreasing (clearly change) the open circuit voltage as noted from (11). In another form, the open circuit voltage can be formed in terms of temperature coefficient K_V of the open circuit voltage, as follow [18, 42]:

$$V_{oc} = V_{oc,STC}\left[1 + K_V \Delta T\right] \tag{12}$$

The temperature coefficient K_V of the open circuit voltage is informed in the datasheet, and it describes the quantity of decreasing of V_{oc} when the temperature is increased.

C. Maximum Power Point

The third important component in the solar PV characteristics is the maximum power point (MPP) which is represented in the *I-V* curve by a point with coordinate $V = V_{mp}$, and $I = I_{mp}$, these values are known as optimum operating voltage and optimum operating current, respectively. The power curve *P-V* is originated from the multiplications of voltage by current ($P = V \times I$). The value of power at short circuit point (0, I_{sc}) is zero, where the voltage at this point equals zero, and the value of power at open circuit voltage point (V_{oc}, 0) is zero, because the current is zero at this point. Between these two points, there is a maximum power somewhere happens, this point is called maximum power point. From (8) the maximum power is given as:

$$P_{max} = V_{mp}\left[I_{sc} - I_{01}\left(e^{\frac{V_{mp}+R_s I_{mp}}{n_1 V_T}} - 1\right) - I_{02}\left(e^{\frac{V_{mp}+R_s I_{mp}}{n_2 V_T}} - 1\right) - \frac{V_{mp} + R_s I_{mp}}{R_{sh}}\right] \tag{13}$$

Since the *I-V* curve is influenced by the internal component of PV device and external factors, then the power curve *P-V* is consequently influenced by those.

D. Fill Factor

The fill factor (*FF*) describes the quality of solar PV modules. It's defined as the ratio of the maximum power output, P_{max}, to the product of open circuit voltage and short circuit current [27, 41]:

$$FF = \frac{P_{max}}{I_{sc}V_{oc}} = \frac{I_{mp}V_{mp}}{I_{sc}V_{oc}} \tag{14}$$

The fill factor has no units, it also can be interpreted graphically as the ratio of rectangular areas (area *A*/area *B*), as shown in Fig. 2.

E. Efficiency of the Solar PV Module

The efficiency of the solar photovoltaic module is defined as the ratio of the output electric power of the PV module to the solar power incident on the solar PV module surface. Input power is represented by the irradiance *G* multiplied by the area of solar PV panel (module), A_{mod}, (it should be noted that $A_{mod} = N_S N_P A_{cell}$). Output power can be taken to be maximum power since the PV panel operated up to its maximum efficiency, then [41]:

$$\eta_{max} = \frac{P_{max}}{GA_{mod}} = FF\,\frac{I_{sc}V_{oc}}{GA_{mod}} \tag{15}$$

where η_{max} is the maximum efficiency of the photovoltaic module. As can be clearly seen from (15) the efficiency of power conversion is proportional to three main parameters: short circuit current, open circuit voltage, and fill factor, for a given solar irradiance.

IV. EFFECT OF PARAMETERS VARIATION ON PV MODULE PERFORMANCE

The most affected factors on PV performance are the irradiance level and temperature, as well as the variations of physical parameters of the solar cell also effect on PV performance. The *I-V* curve of the PV module is sensitive to these variations, and consequently the *P-V* curve is sensitive to those variations. The effects of these parameters on the solar photovoltaic module performance are individually presented in this section.

A. Effect of Solar Irradiation

The I_{sc} of a PV module depends linearly on irradiance level as illustrated in equation (10), and the *I-V* equation (8) depends strongly on I_{sc}, then it can be noted that any variations in irradiation level will cause variations in the output current. i.e. the increase of irradiation will cause an increase in the output current. Unlike short circuit current, the effect of irradiation is not strong on open circuit voltage. From (11) the decrease in short circuit current will cause a very slight decrease in open circuit voltage which depend logarithmically on short circuit current. As the I_{sc} increases due to increasing irradiance level, the power increases accordingly.

B. Effect of Temperature

Solar cell temperature has a strong effect on *I-V* curve characteristics. The increasing of temperature caused increasing the reverse saturation current, and consequently V_{oc} (which is inverse proportional to I_0) will decreases as shown in equation (11). Also, it can be seen from (12) the increasing of cell temperature caused a decrease in open circuit voltage. Whereas the increasing in temperature will cause a very slight increase in the short circuit current as expected in (10). As the open circuit voltage decreases temperature increases, then the power decreases accordingly.

C. Effect of the Series Resistance

Although the fill factor of a solar cell is a useful parameter to evaluate the performance of solar PV device, it can't be expressed explicitly in terms of other PV device parameters. In other words, it can't be clearly seen the effect of physical parameters (such as series resistance) of solar cells on the behaviour of *I-V* curve originated using (8), because it's not an explicit equation. But in general, the series resistance impedes the flow of the output electric current, and accordingly the output power decreases.

D. Effect of Shunt Resistance

For the same reason related to equation (8), it can't be clearly seen the effect of the shunt resistance on the behavior of *I-V* non-linear equation.

E. Effect of Ideality Diode Factor (n_1)

It's also difficult (for the same reason) to know the effect of the ideality diode factor on the behaviour of *I-V* curve. But as general the increasing of n_1 degrades the performance of solar PV module by decreasing the fill factor, therefore the power will decreases accordingly.

F. Effect of Recombination

The equivalent circuit represents recombination by the second diode term, it has a reverse saturation current I_{02} different from the ideal diode, it also has a diode quality factor different to 1 [41], most often diode quality factor is assumed to be closed to 2 [35, 41]. Equation (11) shows that the increase of saturation current will cause a decrease in the open circuit voltage, consequently, the power decreases.

V. PARAMETERS ESTIMATION OF SOLAR PV MODULE

Modelling the performance of the solar PV module requires properly estimating the physical parameters such as shunt (parallel) resistance R_{sh} and series resistance R_s. For the double diode model, several previous studies considered the ideality factors of diodes $n_1 = 1$ and $n_2 = 2$, [9, 19] . Ishaque et al. [19] proposed a modification of equations (6) and (7) to set both I_{01} and I_{02} equal in magnitude, i.e. :

$$I_{01} = I_{02} = \frac{I_{sc,STC} + K_I \Delta T}{\exp\left[\left(V_{oc,STC} + K_V \Delta T\right) \Big/ \left(\frac{n_1 + n_2}{p} V_T\right)\right] - 1} \tag{16}$$

The value of n_1 is recommended to be the unity, and $n_2 \geq 1.2$ [19]. Since $n_1 = 1$, and $\frac{n_1 + n_2}{p} = 1$, it yields that variable $p \geq 2.2$. There are two parameters stay unknown in equation (8), shunt resistance R_{sh}, and series resistance R_s, to establish a model, these parameters must be calculated for predicting the photovoltaic module performance.

In this study R_s and R_{sh} were calculated by Supposing the maximum experimental power obtained from the datasheet $P_{max,e}$ at STC equals the maximum power $P_{max,m}$ estimated using the established model (4) at MPP. The relation between R_s and R_{sh} can be found by applying $P_{max,e} = P_{max,m}$ as follow [9]:

$$P_{max,m} = V_{mp}\left[I_{ph} - I_{01}\left(e^{\frac{V_{mp}+R_s I_{mp}}{n_1 V_t}} - 1\right) - I_{02}\left(e^{\frac{V_{mp}+R_s I_{mp}}{n_2 V_t}} - 1\right) - \frac{V_{mp} + R_s I_{mp}}{R_{sh}}\right] \tag{17}$$

From (17) R_{sh} can be described as [9, 19]:

$$R_{sh} = V_{mp}\left(\frac{V_{mp} + R_s I_{mp}}{V_{mp} I_{ph} - V_{mp} I_{01}\left(e^{\frac{V_{mp}+R_s I_{mp}}{n_1 V_t}} - 1\right) - V_{mp} I_{02}\left(e^{\frac{V_{mp}+R_s I_{mp}}{n_2 V_t}} - 1\right) + V_{mp} I_0 - P_{max,e}}\right) \tag{18}$$

Several iterations using the numerical Newton-Raphson method are required to determine the values of R_s and R_{sh}. The iterative method will continue until $P_{max,e} = P_{max,m}$ (in fact $\varepsilon = |P_{max,e} - P_{max,m}| <$ tolerance). The value of R_s must be started from $R_s = 0$, and slowly incremented until $P_{max,e} = P_{max,m}$. At each iteration, R_{sh} is determined from (18). Initial guesses of R_{sh} may be given by [18, 19]:

$$R_{s0} = 0, \quad R_{sh,min} = \frac{V_{mp}}{I_{sc,STC} - I_{mp}} - \frac{V_{oc,STC} - V_{mp}}{I_{mp}} \tag{19}$$

The mathematical equation (8) of the non-linear *I-V* curve is not an explicit equation, since $V = f(V,I)$ and $I = f(V,I)$. numerical technique such as Newton-Raphson must be applied to solve the non-linear *I-V* equation. it is given as [43]:

$$I_{i+1} = I_i - \frac{f(I_i)}{\dot{f}(I_i)} \tag{20}$$

where, I_i is the i^{th} iteration current, and the $f(I)$ is derivative of the form $f(I)$.

The iterative method algorithm used to calculate the values of R_s and R_{sh} to establish the non-linear *I-V* model is illustrated in Fig. 4 [9, 19].

VI. MODEL VALIDATION

The accuracy of the established model can be examined by comparing its performance with measured data. This can be achieved by using the statistical error tests, such as sum of squared error (SSE), root mean square error (RMSE), and correlation coefficient, R^2. These criteria are given in the following equations [44–50]:

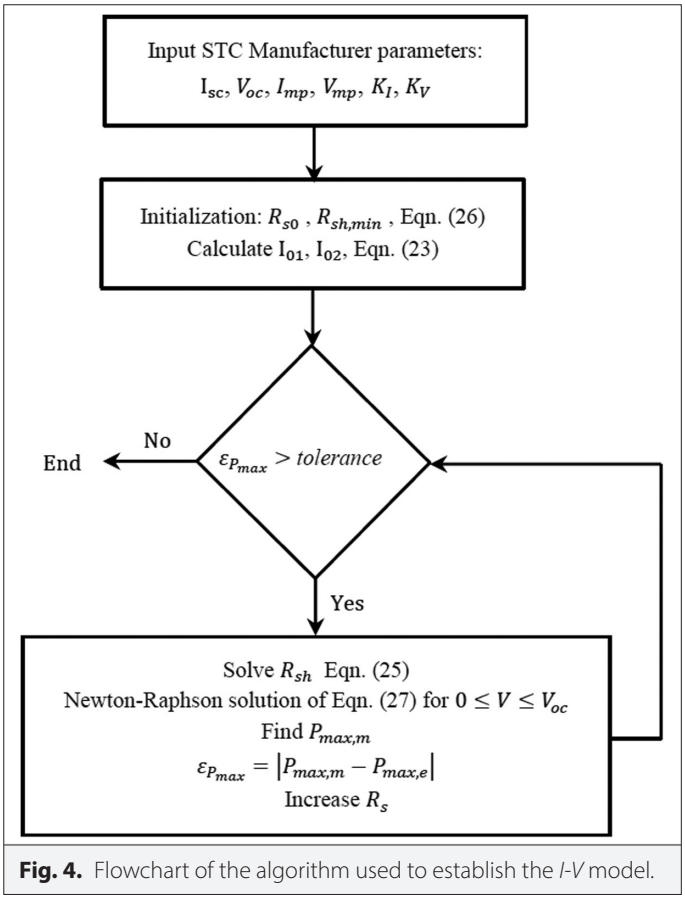

Fig. 4. Flowchart of the algorithm used to establish the *I-V* model.

$$RMSE = \sqrt{\frac{1}{s}\sum_{i=1}^{s}\left(I_{m_i} - I_{e_i}\right)^2} \tag{21}$$

$$SSE = \sum_{i=1}^{s}\left(I_{m_i} - I_{e_i}\right)^2 \tag{22}$$

$$R^2 = \frac{1}{s-1}\sum_{i=1}^{s}\frac{\left(I_{e_i} - \bar{I}_{e_i}\right)\left(I_{m_i} - \bar{I}_{m_i}\right)}{\sigma_e \sigma_m} \tag{23}$$

where, I_{m_i}, I_{e_i} are the i^{th} current values of the mathematical model and the experiment, respectively. $\bar{I}_{m_i}$, $\bar{I}_{e_i}$ denote the mean values of the established current of *I-V* curve and the experimental current, respectively. σ_m, σ_e are the standard deviation of the established current of *I-V* curve and the experimental current, respectively, and *s* is the number of samples. RMSE is useful to know how closely a model fits some measured data, it's a suitable tool to inspect the quality of the fit between estimated and measured data. It measures the average mismatch between each point of measured data and the model. The correlation coefficient describes the correlation between estimated and measured data, its values between -1 (indicates a perfect negative correlation), and 1 (indicates a perfect positive correlation), whereas the value of 0 denotes the two data sets are completely different.

VII, RESULTS AND DISCUSSION

A. Verification of the Model

The electrical and thermal specifications of the polycrystalline KYOCERA KC125GT solar PV module presented in Table I are used to establish *I-V* curve model, where the series and shunt resistances included in equation (4) are calculated by using the iterative method shown in Fig. 4. At each iteration, the error in maximum power $\varepsilon_{P_{max}}$ decreased. When the error is closed to zero, it verifies that $P_{max,m} = P_{max,e}$, thus the iterative method gives the solution $R_s = 0.204\Omega$ and $R_{sh} = 40.523\Omega$. The unknown parameters of the established model are determined at STC based on the characteristics of the mentioned PV module. They are shown in Table II.

The accuracy of the performance of the established model is evaluated by using a comparison of its performance with experimental data provided by the manufacturer datasheet. The panel is made of 36 ($N_s = 36$) PV cells connected in series ($N_p = 1$), and provides 125 W of power at STC. Fig. 5 shows the *I-V* and *P-V* characteristics of the selected panel (module) in combined axes under STC. The three remarkable points $V_{oc} = 21.7V$, $I_{sc} = 8A$, and maximum power point ($P_{max} = 125.3W$, $V_{mp} = 17.4V$, $I_{mp} = 7.2A$) are shown. The *I-V* and *P-V* curves exactly match these remarkable points.

The established model performance accuracy is also tested by comparing its performance with measured data recorded by the PVPM1000C device at the field. The equipment used for the measurement is shown in Fig. 6, which are: reference cell for measuring the solar irradiance and temperature, and solar PV panel, both are set in the same tilt angle and direction. The characteristics of

TABLE II. PARAMETERS OF THE ESTABLISHED MODEL OF THE KC125GT SOLAR PV MODULE AT STC.

I_{mp}	7.2 A
V_{mp}	17.4 V
$P_{max,m}$	125.28 W
I_{sc}	8 A
V_{oc}	21.7 V
I_{01}=I_{02}	5.177×10^{-10} A
R_s	0.204 Ω
R_{sh}	40.523 Ω

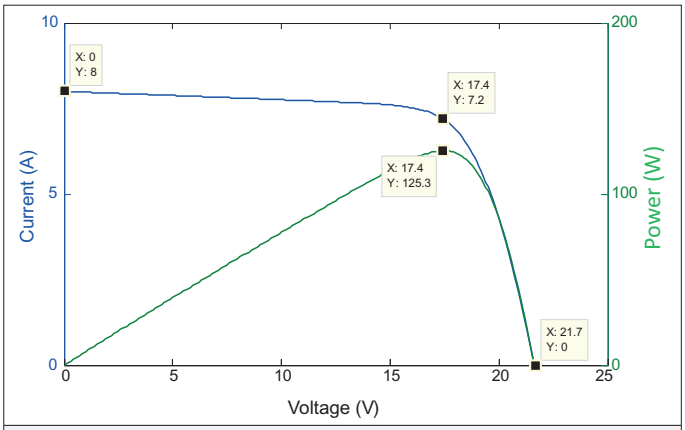

Fig. 5. *I-V* and *P-V* Characteristic of KYOCERA KC125GT solar PV module with three remarkable points at STC.

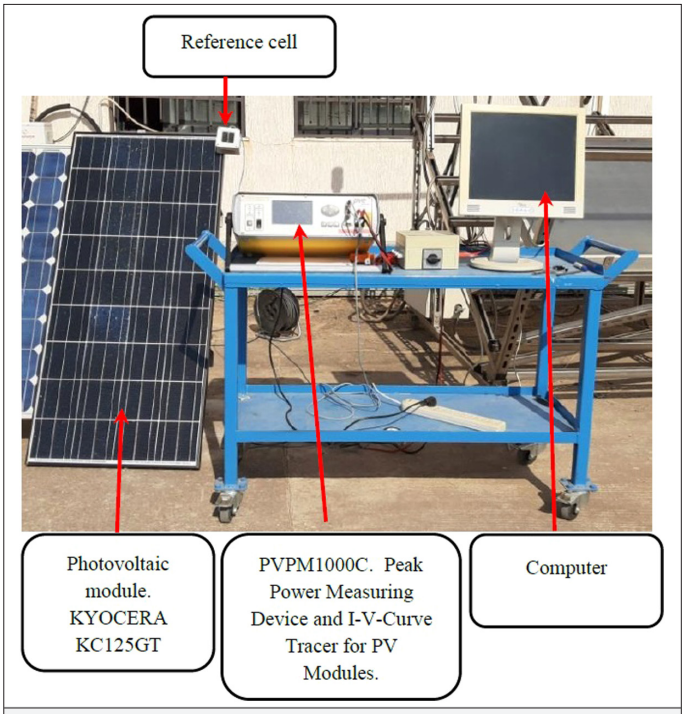

Fig. 6. Outdoor measurement equipment.

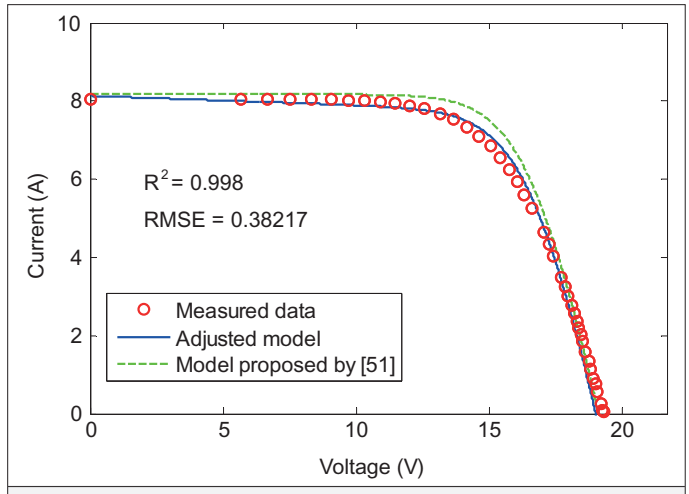

Fig. 7. *I-V* curve of the established model and experimental data, comparison with [51].

I-V and *P-V* curves were recorded by PVPM1000C device, then they transmitted to the computer for analysis. The outdoor weather conditions at execution of the experiment were G=1004 W/m^2 and T=58°C (cell temperature). These conditions are applied to the established model to evaluate its performance. The results are shown in Figs 7 and 8.

Several statistical criteria were used to evaluate the model performance under outdoor test conditions (G=1004 W/m^2 and T=58°C), their values were: SSE=3.7744 A^2, RMSE=0.3822 A, and R^2=0.9980.

In fact, even though the ambient temperature is constant or slightly changed, the increase of irradiance will result in an increase in cell temperature, as clarified in (9). So Fig. 9 gives a prediction of the effect of cell temperature and solar irradiance on the output power harvested from the module under investigation. It shows that, when the temperature axis is fixed at 25oC, the power varies through the irradiance axis from 0 to 125 W. Also when irradiance is fixed at a specified value such as 631.6 W/m^2, the power varies along the temperature axis from 76.98 W to 61.24 W.

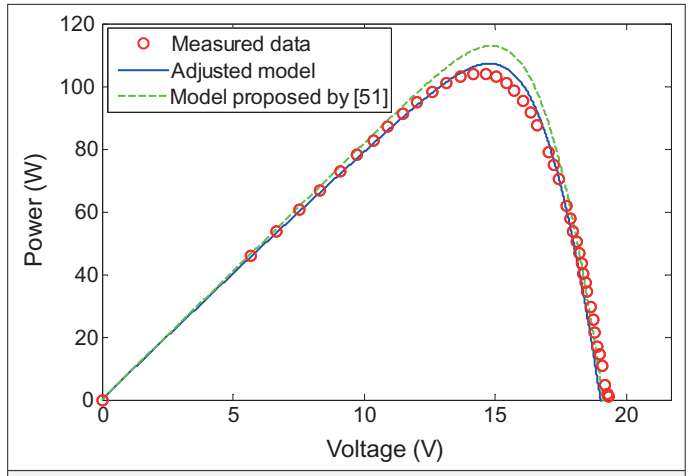

Fig. 8. *P-V* curve of the established model and experimental data, comparison with [51].

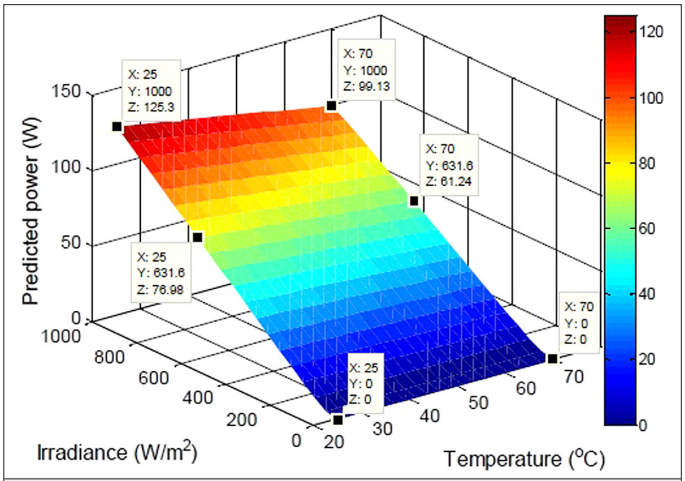

Fig. 9. 3D visualization of predicting the harvested power from the selected module in terms of irradiance and temperature.

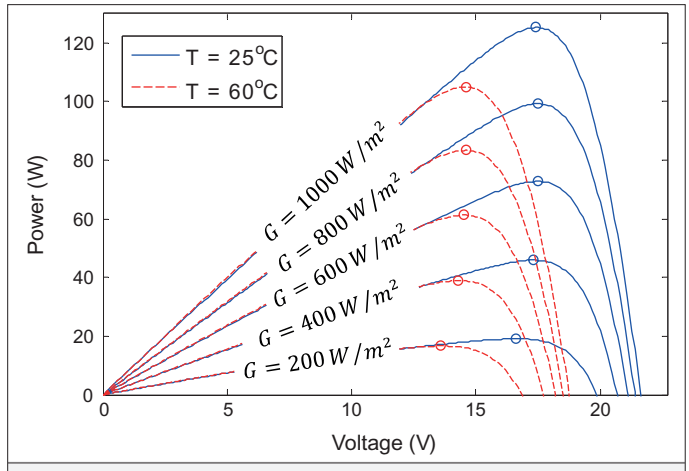

Fig. 11. *P-V* characteristics at various irradiance and temperature.

B. Simulation of the Influence of Environmental and Physical Factors on the Model Performance

The effects of variation of external factors of environment, irradiation and temperature, as well as the internal parameters of PV device on *I-V* and *P-V* curves Based on double-diode model have been simulated. The effect of weather parameters (*G*,*T*) and physical parameters (R_s, R_{sh}, n, I_{02}) on the solar photovoltaic module performance are investigated separately in this study. The variation of irradiance is simulated to know its influence on the performance of solar PV module. Figs. 10 and 11 illustrate in a combined plot the variation effect of both irradiance and temperature on *I-V* and *P-V* curves, respectively. The results shown in Fig. 10 show that the effect of temperature is strong on open circuit voltage, and the effect of irradiance is strong on short circuit current. It is clearly seen from Fig. 10, also as expected from equation (10) that the I_{sc} strongly depends on the irradiance, i.e. the higher the irradiance the larger the short circuit current, which in turn the larger the output power. On the other hand, voltage is not going to vary much. It becomes clear from shown figures and results presented in Table II that one of the most electrical parameters affected by the irradiance level is the short circuit current. It can be observed from Fig. 11 that the decreasing of irradiance level will result in a decrease of maximum power. The simulation result of the *I-V* and *P-V* curves regarding to the influence of temperature is also illustrated in Figs 10 and 11, respectively. As expected from (11) and (12), Fig. 10 shows that the increase of temperature degrades the PV module performance, i.e. the higher the temperature, the lower the V_{oc}, which in turn the lower the maximum output power as shown in Fig. 11. On the other hand, the short circuit current is not going to vary much, and it is almost staying constant. It becomes clear from Figs 10 and 11, that the temperature affects the open circuit voltage more than the short circuit current.

The variation of series resistance is simulated to know its influence on the performance of the PV module by setting the irradiance and temperature under STC, ($G=1000W/m^2$, $T=25°C$), and varying the series resistance ($R_s=0.204\Omega$, 0.5Ω, 1Ω, 1.5Ω). The simulation result of the Characteristics of the *I-V* curve regarding to the mentioned conditions is shown in Fig. 12. It shows that all values of open circuit voltage across the same point in the voltage axis although of variation of series resistance, thus it verifies that, the open circuit voltages are independent of values of series resistance, but as can be seen, the increasing of series resistance value caused a large difference in the *I-V* characteristics. Thus, the increase of series resistance will result in a decrease in power. It can be clearly seen from Fig. 12 that

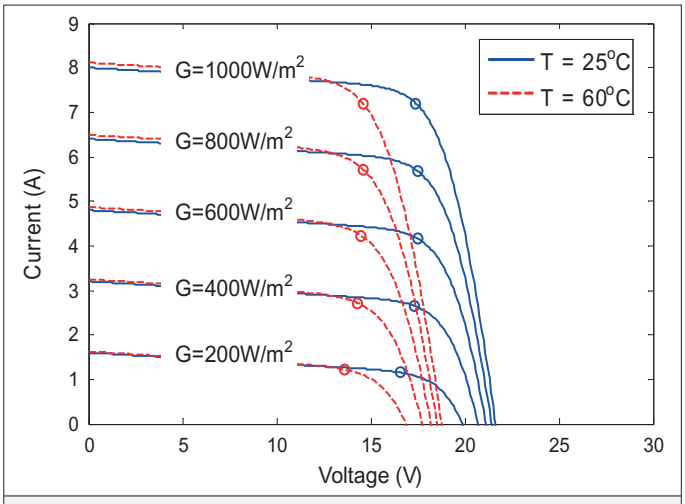

Fig. 10. *I-V* characteristics at various irradiance and temperature.

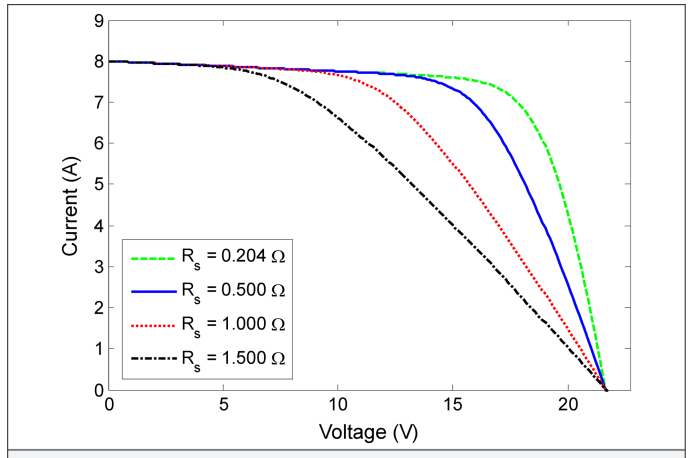

Fig. 12. Effect of series resistance variation on *I-V* characteristics.

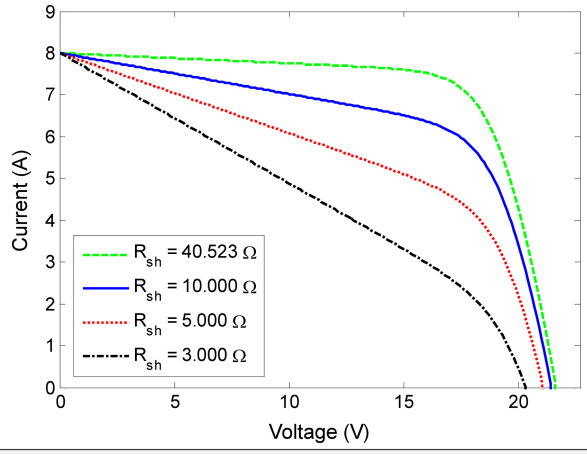

Fig. 13. Effect of shunt resistance variation on *I-V* characteristics.

the most parameter affected by series resistance is the fill factor, thus consequently the output power.

The variation of shunt resistance is simulated to know its influence on the performance of the PV module by setting the irradiance and temperature under STC, ($G=1000W/m^2$, $T=25°C$), and varying the shunt resistance to be ($R_{sh}=40.523\Omega$, 10Ω, 5Ω, 3Ω). The simulation result of the Characteristics of the *I-V* curve according to these conditions is depicted in Fig. 13. The results shown in the figure show that the open circuit voltage is slightly modified as shunt resistance decreases, i.e. the decrease of shunt resistance will cause a slightly decrease in the open circuit voltage. The maximum power is influenced by shunt resistance, i.e. the higher the R_{sh}, the greater the power and *FF*. It can be clearly seen that the most parameter affected by shunt resistance is the fill factor, and consequently the maximum power.

The variation of the diode ideality factor is simulated to know its influence on the performance of the PV module by setting the irradiance and temperature under STC, ($G=1000W/m^2$, $T=25°C$), and varying the diode ideality factor to be ($n_1=1$, 1.4, 1.8, 2.5). The simulation result of the Characteristics of *I-V* curve according to these conditions is illustrated in Fig. 14. It becomes clear from the shown results

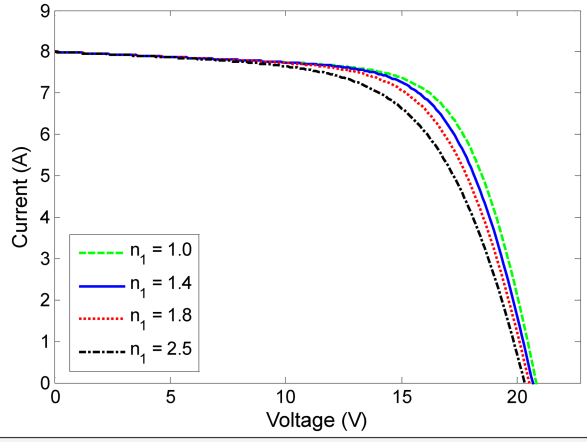

Fig. 14. Effect of diode ideality factor (n_1) variation on *I-V* characteristics.

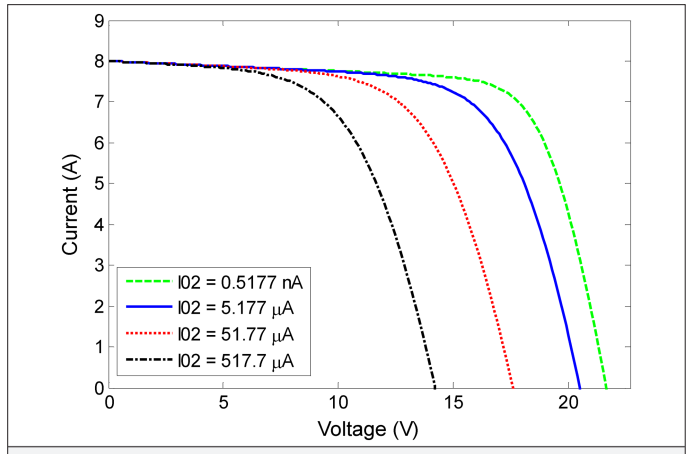

Fig. 15. Effect of recombination diode (I_{02}) variation on *I-V* characteristics.

that one of the most electrical parameters affected by the diode ideality factor is the fill factor. Fig. 14 illustrates a slightly reduction of open circuit voltage as the diode ideality factor increases. The maximum power is influenced by n_1, i.e. the lower the, the greater the power and *FF*.

The variation of recombination diode (reverse saturation current of the second diode, I_{02}) is simulated to know its influence on the performance of the solar PV module by setting the irradiance and temperature under STC, ($G=1000W/m^2$, $T=25°C$), and varying the recombination diode to be ($I_{02}=5.177\times10^{-9}$, 5.177×10^{-6}, 51.77×10^{-6}, 0.5177×10^{-3} A). The simulation result of the *I-V* curve characteristics under the mentioned conditions is shown in Fig. 15. The results indicate that, when recombination diode increases, the open circuit voltage heavily decreased, and consequently the maximum power is degraded, and the short circuit current remains constant.

VIII. CONCLUSION

In this study, a mathematical model was established based on double diode equivalent circuit to describe the performance of solar PV module, also to predict the performance under different weather conditions. The model parameters were estimated using the numerical Newton-Raphson method. Measured data of KYOCERA KC125GT solar PV panel (module) recorded at the field were used to validate the established model. The accuracy of the established model is evaluated using statistical error tests such as correlation coefficient, absolute error, and root mean square error. The results showed a good agreement between measured data and the established model. The effect of weather conditions on the performance of the mentioned solar PV module was simulated using the established model. It can be concluded that:

- The effect of irradiance is strong on short circuit current, and the effect of temperature is strong on the open circuit voltage.
- The short circuit current depends strongly on solar irradiance. The higher the irradiance the larger the short circuit current, which in turn the larger the harvested power, whereas, the open circuit voltage is not going to vary much.
- The increase in temperature decreases the open circuit voltage, and the maximum output power degrades accordingly. whereas, the short circuit current almost remains constant.

- The most parameter affected by series and shunt resistances is the fill factor, and consequently the output power. The fill factor decreases at increasing series resistance and decreasing shunt resistance.
- The increase in reverse saturation current of the second diode decreases the open circuit voltage heavily, and consequently the output maximum power.

Peer-review: Externally peer-reviewed.

Author Contributions: Concept - A.T., A.J.; Design - A.T., A.J.; Materials - A.T.; Data Collection and/or Processing - A.T.; Analysis and/or Interpretation - A.T.; Literature Review - A.T., A.J.; Writing - A.T.; Critical Review - A.T., A.J.

Declaration of Interests: The authors declare that they have no competing interest.

Funding: The authors declared that this study has received no financial support.

REFERENCES

1. T. Salmi, M. Bouzguenda, A. Gastli, and A. Masmoudi, "MATLAB/simulink based modeling of photovoltaic cell," *Int. J. Renew. Energy Res. (IJRER)*, vol. 2, no. 2, pp. 213–218, 2012.
2. R. Kumar, and R. Muralidharan, "Mathematical modeling, simulation, and validation of photovoltaic cells," *Int. J. Res. Eng. Technol. (IJRET)*, vol. 3, no. 10, pp. 170–174, 2014.
3. J. M. Álvarez *et al.*, "Analytical modeling of current-voltage photovoltaic performance: An easy approach to solar panel behavior," *Appl. Sci.*, vol. 11, no. 9, p. 4250, 2021. [CrossRef]
4. A. Şentürk, "New method for computing single diode model parameters of photovoltaic modules," *Renew. Energy*, vol. 128, pp. 30–36, 2018. [CrossRef]
5. C. S. Ruschel, F. P. Gasparin, and A. Krenzinger, "Experimental analysis of the single diode model parameters dependence on irradiance and temperature," *Sol. Energy*, vol. 217, pp. 134–144, 2021. [CrossRef]
6. A. K. Abdulrazzaq, G. Bognár, and B. Plesz, "Accurate method for PV solar cells and modules parameters extraction using I–V curves," *J. King Saud Univ. Eng. Sci.*, vol. 34, no. 1, 46–56, 2022. [CrossRef]
7. A. Gholami, M. Ameri, M. Zandi, and R. G. Ghoachani, "A single-diode model for photovoltaic panels in variable environmental conditions: Investigating dust impacts with experimental evaluation," *Sustain. Energy Technol. Assess.*, vol. 47, p. 101392, 2021. [CrossRef]
8. A. Yahya-Khotbehsara, and A. Shahhoseini, "A fast modeling of the double-diode model for PV modules using combined analytical and numerical approach" *Sol. Energy*, vol. 162, pp. 403–409, 2018. [CrossRef]
9. K. Ishaque, Z. Salam, and H. Taheri, "Simple, fast and accurate two-diode model for photovoltaic modules," *Sol. Energy Mater. Sol. Cells*, vol. 95, no. 2, pp. 586–594, 2011. [CrossRef]
10. S. Shongwe, and Moin Hanif, "Comparative analysis of different single-diode PV modeling methods," *IEEE J. Photovolt.*, vol. 5, no. 3, pp. 938–946, 2015. [CrossRef]
11. A. Chatterjee, A. Keyhani, and D. Kapoor, "Identification of photovoltaic source models," *IEEE Trans. Energy Convers.*, vol. 26, no. 3, pp. 883–889, 2011. [CrossRef]
12. F. Ghani, G. Rosengarten, M. Duke, and J. K. Carson, "The numerical calculation of single-diode solar-cell modelling parameters," *Renew. Energy*, vol. 72, pp. 105–112, 2014. [CrossRef]
13. D. Ben hmamou *et al.*, "Parameters identification and optimization of photovoltaic panels under real conditions using Lambert W-function," *Energy Rep.*, vol. 7, pp. 9035–9045, 2021. [CrossRef]
14. H. Fathabadi, "Lambert W function-based technique for tracking the maximum power point of PV modules connected in various configurations," *Renew. Energy*, vol. 74, pp. 214–226, 2015. [CrossRef]
15. A. A. El-Fergany, "Parameters identification of PV model using improved slime mould optimizer and Lambert W-function," *Energy Rep.*, vol. 7, pp. 875–887, 2021. [CrossRef]
16. J. Polo *et al.*, "Modeling IV curves of photovoltaic modules at indoor and outdoor conditions by using the Lambert function," *Energy Convers. Manag.*, vol. 195, pp. 1004–1011, 2019. [CrossRef]
17. M. Ćalasan, S. H. E. Abdel Aleem, and A. F. Zobaa, "A new approach for parameters estimation of double and triple diode models of photovoltaic cells based on iterative Lambert W function," *Sol. Energy*, vol. 218, pp. 392–412, 2021. [CrossRef]
18. M. G. Villalva, J. R. Gazoli, and E. R. Filho, "Comprehensive approach to modeling and simulation of photovoltaic arrays," *IEEE Trans. Power Electron.*, vol. 24, no. 5, pp. 1198–1208, 2009. [CrossRef]
19. K. Ishaque, Z. Salam, H. Taheri, and Syafaruddin, "Modeling and simulation of photovoltaic (PV) system during partial shading based on a two-diode model," *Simul. Modell. Pract. Theor.*, vol. 19, no. 7, pp. 1613–1626, 2011. [CrossRef]
20. A. El-Tayyan, "PV system behavior based on datasheet," *J. Electron. Dev.*, vol. 9, pp. 335–341, 2011.
21. S. Alsadi, and B. Alsayid, "Maximum power point tracking simulation for photovoltaic systems using perturb and observe algorithm," *Int. J. Eng. Innov. Technol. (IJEIT)*, vol. 2, no. 6, pp. 80–85, 2012.
22. H. Bellia, R. Youcef, and M. Fatima, "A detailed modeling of photovoltaic module using MATLAB," *NRIAG J. Astron. Geophys.*, vol. 3, no. 1, pp. 53–61, 2014. [CrossRef]
23. S. M. Salih, F. F. Salih, M. L. Hasan, and M. Y. Bedaiawi, "Performance evaluation of photovoltaic models based on a solar model tester," *IJITCS*, vol. 4, no. 7, pp. 1–10, 2012. [CrossRef]
24. A. McEvoy, L. Castaner, and T. Markvart, *Solar Cells: Materials, Manufacture and Operation*. Academic Press Is an Imprint of Elsevier, 2013. https://books.google.com.ly/books?hl=en&lr=&id=g5ppmHYfNAoC&oi=fnd&pg=PP1&dq=McEvoy,+Augustin,+Luis+Castaner,+and+Tom+Markvart.+Solar+cells:+materials,+manufacture+and+operation&ots=nCh-_CTsdk&sig=nVYM8XgsKkHoqIW94V2hM5hKtb8&redir_esc=y#v=onepage&q=McEvoy%2C%20Augustin%2C%20Luis%20Castaner%2C%20and%20Tom%20Markvart.%20Solar%20cells%3A%20materials%2C%20manufacture%20and%20operation&f=false. https://www.amazon.com/s?k=Solar+Cells%3A+Materials%2C+Manufacture+and+Operation&crid=3MJ67ISY0HVKR&sprefix=solar+cells+materials%2C+manufacture+and+operation%2Caps%2C253&ref=nb_sb_noss
25. A. M. Humada, M. Hojabri, S. Mekhilef, and H. M. Hamada, "Solar cell parameters extraction based on single and double-diode models: A review," *Renew. Sustain. Energy Rev.*, vol. 56, pp. 494–509, 2016. [CrossRef]
26. T. Easwarakhanthan, J. Bottin, I. Bouhouch, and C. Boutrit, "Nonlinear minimization algorithm for determining the solar cell parameters with microcomputers," *Int. J. Sol. Energy*, vol. 4, no. 1, pp. 1–12, 1986. [CrossRef]
27. S. Wenham, M. Green, M. Watt, and R. Corkish, *Applied Photovoltaics*. Earthscan Publications, 2007. https://www.taylorfrancis.com/books/mono/10.4324/9781849776981/applied-photovoltaics-stuart-wenham-martin-green-muriel-watt-richard-corkish-alistair-sproul https://books.google.com.ly/books?id=cP_FxlQ1fCEC&printsec=frontcover&dq=Book++Applied+Photovoltaics++Wenham,&hl=en&sa=X&ved=2ahUKEwiHhIaVhtj4AhXdlP0HHWqbAOUQ6AF6BAgJEAI#v=onepage&q=Book%20%20Applied%20Photovoltaics%20%20Wenham%2C&f=false.
28. D. Neamen, *Electronic Circuit Analysis and Design*. New York, United States of America: McGraw-Hill, 2001.
29. D. S. H. Chan, J. R. Phillips, and J. C. H. Phang, "A comparative study of extraction methods for solar cell model parameters," *Solid State Electron.*, vol. 29, no. 3, pp. 329–337, 1986. [CrossRef]
30. J. C. H. Phang, D. S. H. Chan, and J. R. Phillips, "Accurate analytical method for the extraction of solar cell model parameters," *Electron. Lett.*, vol. 20, no. 10, pp. 406–408, 1984. [CrossRef]
31. Y. Mahmoud, W. Xiao, and H. H. Zeineldin, "A simple approach to modeling and simulation of photovoltaic modules," *IEEE Trans. Sustain. Energy*, vol. 3, no. 1, pp. 185–186, 2012. [CrossRef]
32. J. Bai, Y. Cao, Y. Hao, Z. Zhang, S. Liu, and F. Cao, "Characteristic output of PV systems under partial shading or mismatch conditions," *Sol. Energy*, vol. 112, pp. 41–54, 2015. [CrossRef]
33. M. Seyedmahmoudian, S. Mekhilef, R. Rahmani, R. Yusof, and E. Renani, "Analytical modeling of partially shaded photovoltaic systems," *Energies*, vol. 6, no. 1, pp. 128–144, 2013. [CrossRef]
34. T. R. Ayodele, A. S. O. Ogunjuyigbe, and E. E. Ekoh, "Evaluation of numerical algorithms used in extracting the parameters of a single-diode

photovoltaic model," *Sustain. Energy Technol. Assess.*, vol. 13, pp. 51–59, 2016. [CrossRef]
35. D. Chan, and J. Phang, "Analytical methods for the extraction of solar-cell single-and double-diode model parameters from IV characteristics," *IEEE Trans. Electron Devices*, pp. 286–293, 1987.
36. B. Alsayid, "Modeling and simulation of photovoltaic cell/module/array with two-diode model," *Int. J. Comput. Technol. Electron. Eng. (IJCTEE)*, vol. 1, no. 3, pp. 6–11, 2012.
37. M. Hejri, H. Mokhtari, M. R. Azizian, M. Ghandhari, and L. Söder, "On the parameter extraction of a five-parameter double-diode model of photovoltaic cells and modules," *IEEE J. Photovolt.*, vol. 4, no. 3, pp. 915–923, 2014. [CrossRef]
38. R. Kadri, H. Andrei, J. Gaubert, T. Ivanovici, G. Champenois, and P. Andrei, "Modeling of the photovoltaic cell circuit parameters for optimum connection model and real-time emulator with partial shadow conditions," *Energy*, vol. 42, no. 1, pp. 57–67, 2012. [CrossRef]
39. C. Morcillo-Herrera, F.Hernández-Sánchez, and M. Flota-Bañuelos, "Practical method to estimate energy potential generated by photovoltaic cells: Practice case at Merida City," *Energy Procedia*, vol. 57, pp. 245–254, 2014. [CrossRef]
40. T. A. Olukan, and M. Emziane, "A comparative analysis of PV module temperature models," *Energy Procedia*, vol. 62, pp. 694–703, 2014. [CrossRef]
41. L. Castaner, and S. Silvestre, *Modelling Photovoltaic Systems Using PSpice*. Chichester: John Wiley and Sons, 2002.
42. V. Perraki, and P. Kounavis, "Effect of temperature and radiation on the parameters of photovoltaic modules," *J. Renew. Sustain. Energy*, vol. 8, no. 1, p. 013102, 2016. [CrossRef]
43. S. Chapra, and R. Canale, *Numerical Methods for Engineers*, 6th ed. McGraw-Hill, 2010. https://books.google.com.ly/books?id=SA1LPgAACAAJ&dq=Numerical+Methods+for+Engineers,+Sixth+Edition+6th+Edition&hl=en&sa=X&ved=2ahUKEwi-7vOPtdf4AhUBRBoKHbLXDYkQ6AF6BAgDEAI https://www.amazon.com/Numerical-Methods-Engineers-Steven-Chapra/dp/0073401064/ref=sr_1_1?crid=2X6SD59LA5KI3&keywords=Numerical+Methods+for+Engineers+6th+Edition&qid=1656668311&s=books&sprefix=numerical+methods+for+engineers+6th+edition%2Cstripbooks-intl-ship%2C215&sr=1-1
44. A. A. Teyabeen, "Statistical analysis of wind speed data," 6th International Renewable Energy Congress (IREC). IEEE Publications, 2015, pp. 1–6. https://ieeexplore.ieee.org/document/7110866.
45. A. A. Teyabeen, F. Akkari, and A. Jwaid, "Comparison of seven numerical methods for estimating Weibull parameters for wind energy applications," In Computer Modelling & Simulation (UKSim), 2017 UKSim-AMSS 19th International Conference on. IEEE Publications, 2017, pp. 173–178. https://ieeexplore.ieee.org/abstract/document/8359062.
46. A. A. Teyabeen, F. R. Akkari, and A. E. Jwaid, "Power curve modelling for wind turbines," In UKSim-AMSS 19th International Conference on, In Computer Modelling & Simulation (UKSim). IEEE Publications, 2017, pp. 179–184. https://ieeexplore.ieee.org/abstract/document/8359063.
47. A. A. Teyabeen, F. R. Akkari, and A. E. Jwaid, "Mathematical modelling of wind turbine power curve," *Int. J. Simul. Syst. Sci. Technol.*, vol. 19, no.5, pp. 1–13, 2018. [CrossRef]
48. A. A. Teyabeen, N. B. Elhatmi, A. A. Essnid, and A. E. Jwaid, "Parameters estimation of solar PV modules based on single-diode model," In 11th International Renewable Energy Congress (IREC). IEEE Publications, 2020, pp. 1–6. https://ieeexplore.ieee.org/abstract/document/9310365.
49. Taha B. M. J. Ouarda, C. Charron, and F. Chebana, "Review of criteria for the selection of probability distributions for wind speed data and introduction of the moment and L-moment ratio diagram methods, with a case study," *Energy Convers. Manag.*, vol. 124, pp. 247–265, 2016. [CrossRef]
50. A. A. Teyabeen, N. B. Elhatmi, A. A. Essnid, and F. Mohamed, "Comparison of seven empirical models for estimating monthly global solar radiation,(case study: Libya)," In 12th International Renewable Energy Congress (IREC). IEEE Publications, 2021, pp. 1–6. https://ieeexplore.ieee.org/abstract/document/9624843.
51. G. Walker, "Evaluating MPPT converter topologies using a MATLAB PV model," *J. Electr. Electron. Eng. Aust.*, vol. 21, no. 1, pp. 49–55, 2001.

Alhassan Ali Teyabeen received the B.Sc. degree in Electrical and Electronics Engineering in 2008 from Misurata University, Libya, and he received the M.Sc. degree in Electrical and Electronics Engineering in 2017 from University of Tripoli, Libya. His current research interests include photovoltaic energy systems, wind energy systems, artificial intelligence applied to photovoltaic and wind energy. He has authored many papers published in international journal and international conferences.

Ali Elseddig Jwaid received the B.Sc. degree in electrical and electronics engineering in 2008 from university of Misurata, Libya. He received the M.Sc. degrees in computer and communication engineering in 2011 from Nottingham Trent University, Nottingham, UK. He received currently the Ph.D. degree in department of computing and technology in 2016 from university of Nottingham Trent, UK. His current research interests include data science for IoT, in healthcare, renewable energy and STEM teaching and learning. He is a Senior Lecturer in faculty of computing, engineering and media at De Montfort University, UK. Also, he is the Program Leader of IoT courses. He has authored or co-authored many technical papers published in international journals and conferences.